Turkish Journal of Electrical Engineering & Computer Sciences

http://journals.tubitak.gov.tr/elektrik/

Research Article

Turk J Elec Eng & Comp Sci
(2013) 21: 1871 – 1879

doi:10.3906/elk-1204-10

Adaptive detection of chaotic oscillations in ferroresonance using modified extended Kalman filter

Cengiz Polat UZUNOĞLU,* Mukden UĞUR
Department of Electrical & Electronics Engineering, Faculty of Engineering, İstanbul University, Avcılar, İstanbul, Turkey

Received: 04.04.2012 • **Accepted:** 20.06.2012 • **Published Online:** 24.10.2013 • **Printed:** 18.11.2013

Abstract: Power quality and power disturbances have become an important factor for power systems. Chaotic ferroresonance is one of the disturbances that may cause overvoltages and overcurrents; hence, it can endanger the system reliability and continuous safe operating. A power system that generates chaotic oscillations is a dynamic system, which can be modeled with a Duffing equation. This paper introduces the application of a modified extended Kalman filter for improving the detection of chaotic behavior of power system signals. A modification algorithm is used to increase the estimation performance of the former casual extended Kalman filter. The proposed method is employed to distinguish the abnormalities from a signal contaminated with chaotic ferroresonance for promoting efficiency in power system characteristics detection.

Key words: Ferroresonance, Duffing oscillator, chaos, extended Kalman filter

1. Introduction

Ferroresonance is initiated by improper switching operation in electrical distribution systems involving nonlinear transformers and capacitors [1]. Due to the transformers saturable inductance and the capacitive effect of the distribution lines, ferroresonance can cause unpredictable overvoltages and high currents in power systems. The ferroresonance appears after transient disturbances or switching operations that manifest as chaotic oscillations and may produce extremely dangerous consequences. Since the ferroresonance phenomenon depends on many other factors and conditions of the power system, ferroresonance continues to be a complex and difficult problem to detect and predict due to its chaotic behavior [2].

Four different types of ferroresonance modes, fundamental ferroresonance, subharmonic ferroresonance, quasiperiodic ferroresonance, and chaotic ferroresonance, can be detected. The quasiperiodic ferroresonance and chaotic ferroresonance are nonperiodic modes. Sudden jumps (bifurcation) may occur when a system causes a sudden change in its behavior from one mode to another [3,4]. In order to define these modes, the nonlinear differential equations solutions (attractors) of a power system containing electromagnetic circuits must be realized [5].

One of the simple oscillator models, which is able to exhibit a chaotic behavior, is the forced Duffing oscillator (FDO). In order to analyze chaotic oscillations caused due to ferroresonance in a power system, forced Duffing equation solutions can be used to describe and simulate a dynamic system model [6]. In this paper, we have used the differential equation that describes the FDO, operating in chaotic mode [7]. This model

*Correspondence: polat@istanbul.edu.tr

was employed to determine and display waveforms including flux, currents, and voltages, as well as Poincaré maps and phase space diagrams for the FDO solution, which initiates ferroresonance conditions. Chaotic ferroresonance may influence and harm power system insulators [8]. In order to eliminate the harmful effects, the power system signal should be monitored continuously.

Due to the fast convergence and increased precision of the estimator, the extended Kalman filter (EKF) can be employed to estimate and detect the ferroresonance phenomenon in a power system [4]. In this paper, the modified EKF (MEKF) is proposed as a novel method to increase the performance. The modification algorithm adjusts the noise variances of the state variables according to the estimation performance [9]. The performance comparisons of both the MEKF and EKF methods are given for different ferroresonance scenarios.

2. Forced Duffing oscillator

Nonlinear oscillator systems are prone to exhibit a chaotic behavior. The influence of external forces on these nonlinear systems may alter the dynamical behavior of power systems dramatically and cause chaotic ferroresonance. The FDO is a simple model that is able to display some of those properties. The most general differential equation of the FDO system is given as follows:

$$\ddot{x} + \delta\dot{x} + (\beta x^3 \pm w_0^2 x) = \gamma\cos(wt + \Phi). \tag{1}$$

This general equation can take various forms depending on the parameter values. In the equation, δ is the damping parameter, γ is the forcing parameter, and w is the angular frequency. Moreover, Φ is the phase of the system and β and w_0 are constants that define the characteristics of the oscillator [10,11]. In the proposed study, the parameters are selected as $\beta = \mathrm{w}_0 = 1$ and $\Phi = 0$ to simulate the chaotic ferroresonance.

$$\ddot{x} + \delta\dot{x} + x^3 - x = \gamma\cos(wt) \tag{2}$$

The ordinary differential equation form of the system is given in Eq. (3).

$$\dot{x} = y, \qquad \dot{y} = x - x^3 - \delta y + \gamma\cos(wt) \tag{3}$$

In the unforced case (the oscillator operates as a regular oscillator), the forcing parameter goes to 0 and the equation takes the following form [11]:

$$\dot{x} = y, \qquad \dot{y} = x - x^3 - \delta y. \tag{4}$$

It is possible to derive different cases by changing the values of these parameters. The simulated chaotic output of the FDO is given in Figure 1. The characteristics of the FDO can be analyzed by the phase space diagram and the Poincaré map. The phase space diagram is an attractor that defines the chaoticness of the model. The Poincaré map also displays the 3-dimensional intersection points of the phase space diagram. Both of these figures represent the fractal behavior. The corresponding phase space diagram and the Poincaré map of the FDO are given in Figure 2.

In order to obtain a proper comparison for the proper working mode of the oscillator, the undamped and unforced oscillator characteristics are analyzed. The regular power system signal can be simulated with the output of the undamped and unforced oscillator, which is given in Figure 3. The corresponding phase space diagram and the Poincaré map of the undamped and unforced oscillator are given in Figure 4.

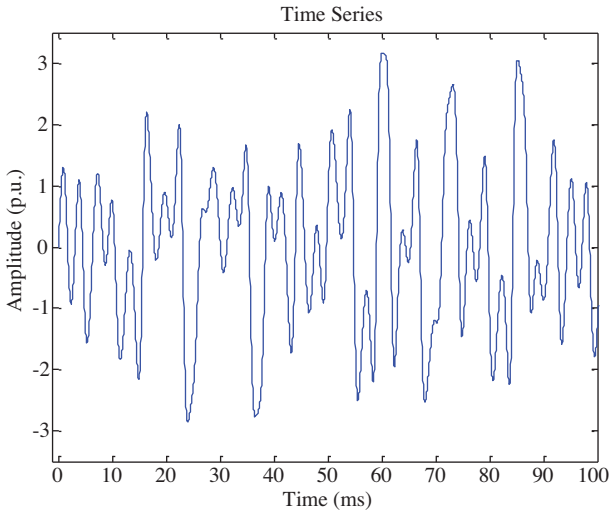

Figure 1. The chaotic time series output of the FDO for $\gamma = 1.5$ and $\delta = 0$.

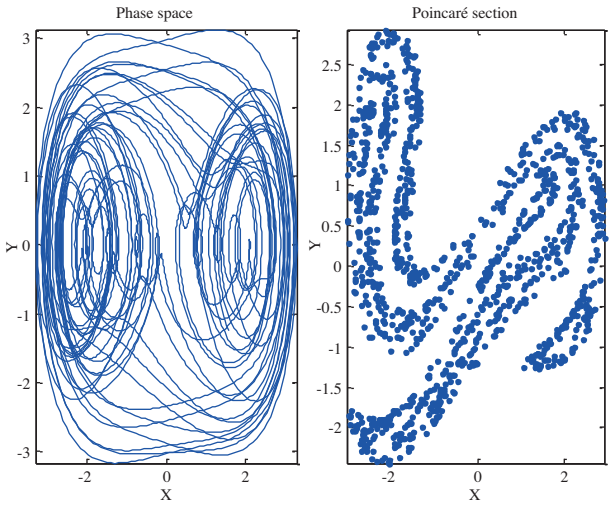

Figure 2. The phase space diagram and the Poincaré map of the FDO for $\gamma = 1.5$ and $\delta = 0$.

In this work, the chaotic mode of the FDO was used to simulate the ferroresonance. The chaotic time series output of the oscillator was handled as a noise component for the power system signal. In order to define the power system frequency accurately, the elimination of the chaotic oscillations of the FDO is vital for the system.

In the unforced case of a Duffing oscillator (UDO), the driving force γ is taken as 0. The δ parameter defines the damping time of the UDO. The simulated damping time series output of the UDO is given in Figure 5. The phase space diagram and the Poincaré map of the damping simulation of the UDO is shown in Figure 6, which does not display the chaotic attractor characteristics as expected. The phase space diagram represents the damping characteristics of the UDO.

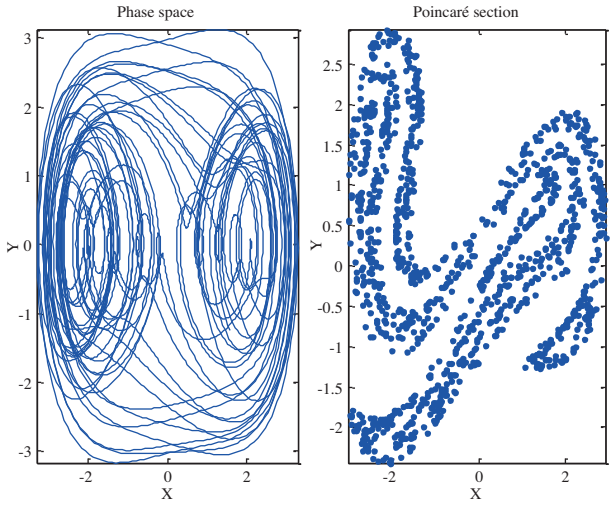

Figure 3. Unforced and undamped UDO output (the power system signal).

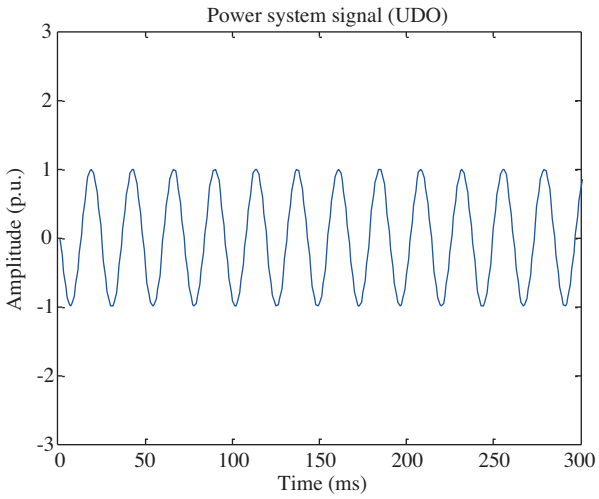

Figure 4. The phase space diagram and the Poincaré map of the unforced and undamped DO.

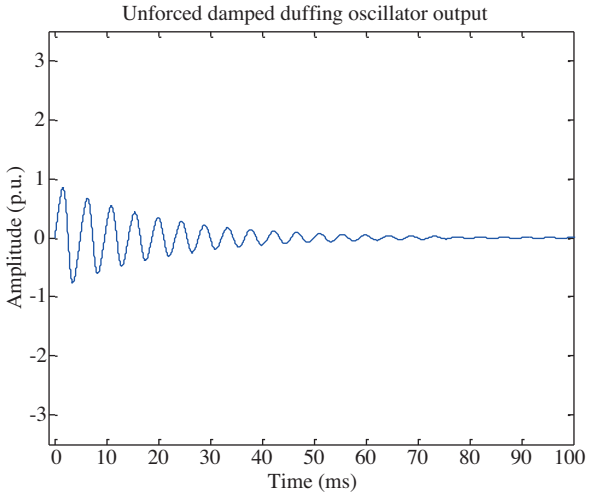

Figure 5. The time series output of the UDO for $\gamma = 0$ and $\delta = 0.2$.

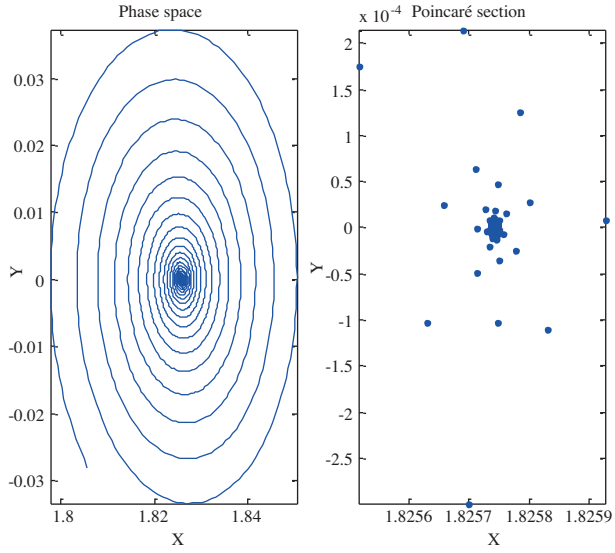

Figure 6. The phase space diagram and the Poincaré map of the UDO for $\gamma = 0$ and $\delta = 0.2$.

2.1. Modified extended Kalman filter

Generally, the EKF is employed for estimating the unknown parameters of a system with corrupted measurements. The chaotic power system signal can be described with a nonlinear state space model. An observation signal z_k at time t_k can be denoted as a sum of x_k of the sinusoids with additive noise v_k.

$$z_k = x_k + v_k, \qquad k = 1, 2, ...N, \tag{5}$$

where

$$x_k = a\cos\left(wt_k + \Phi\right), \tag{6}$$

$$w = 2\pi f. \tag{7}$$

The parameters α, f, and Φ are the amplitude, frequency, and the phase of the power system signal, respectively. In our present study, the observation noise v_k was modeled as the chaotic output of the FDO. In the dynamic system model of the EKF, Eq. (8) represents the state model and Eq. (8) represents the observation (measurement) model [9].

$$x_k = Ax_{k-1} + Bu_k + w_{k-1} \tag{8}$$

$$z_k = Hx_k + v_k \tag{9}$$

In the model, x_k is the state vector, which is the power system signal to be estimated in the EKF algorithm. U_k is the control signal, which is assumed to be 0. The w_{k-1} and v_k are the process and measurement noises, respectively. In the model, A represents the state transition, H represents the observation, and B represents the control matrix. For the EKF model, the relation between the estimated signal and the previously estimated signal is given in Eq. (10).

$$\hat{x}_k = K_k Z_k + (1 - K_k)\,\hat{x}_{k-1} \tag{10}$$

The most important parameter of the filter is the Kalman gain (K_k), which updates the equation to the desired estimation level. Two different groups of equations are used to implement the EKF. The first group is called prediction (time update) equations and this is given in Eqs. (11) and (12):

$$\hat{x}_k^- = A\hat{x}_{k-1}, \tag{11}$$

$$P_k^- = AP_{k-1}A^T + Q. \tag{12}$$

The second group is called correction (observation update) equations and this is given in Eqs. (13) through (15):

$$K_k = P_k^- H^T \left(HP_k^- H^T + R\right)^{-1}, \tag{13}$$

$$\hat{x}_k = \hat{x}_k^- + K_k \left(z_k - H\hat{x}_k^-\right), \tag{14}$$

$$P_k = \left(1 - K_k H\right) P_k^-. \tag{15}$$

In the model, P_k is the error covariance matrix, Q is the process noise covariance matrix, and R is the measurement noise covariance matrix. Before the correction step, the a priori estimations ($\hat{x}_k^-$ and P_k^-) are calculated using the prediction equations. Next, the updated a posteriori estimations ($\hat{x}_k^-$ and P_k^-) are obtained by substituting the a priori estimations into the correction equations. This update process continues iteratively between the prediction and correction steps [8].

2.2. Modification algorithm

In this study, the MEKF is proposed for the estimation of the desired signal. With the modification algorithm, the estimation performance of the EKF is increased. The modification of the EKF depends on the lock detection algorithm [12]. The process noise covariance Q can be represented in the following form:

$$Q_k = \begin{bmatrix} \sigma_{w1}^2 & 0 \\ 0 & \sigma_{w2}^2 \end{bmatrix}, \tag{16}$$

where $\sigma^2 w_1$ and $\sigma^2 w_2$ are Gaussian random variables. The modification algorithm adjusts the covariance matrix Q adaptively according to the tracking performance of the EKF. If the estimation performance is satisfactory, $\sigma^2 w_1$ and $\sigma^2 w_2$ are set to 0. Otherwise, the values are defined by the modification algorithm.

$$\begin{aligned} &\sigma_{w1}^2 = \sigma_{w2}^2 = 0 \qquad \text{as} \quad \tfrac{1}{M}\sum_{m=1}^{M} e_m \geq \gamma.\sqrt{R_k} \\ &\sigma_{w1}^2 = \sigma_{w2}^2 = f_k^2/12 \qquad \text{as} \quad \tfrac{1}{M}\sum_{m=1}^{M} e_m < \gamma.\sqrt{R_k} \end{aligned} \tag{17}$$

The estimation performance is defined by the error function, which is denoted by e. In the equation, γ is a constant with a predefined threshold value and f_k is the frequency of the system signal. This modification improves the performance of the estimation by reducing the convergence time and the estimation error [9]. Using this novel modification algorithm, the EKF operates more efficiently.

3. Simulation results

Computer simulations are carried out for a 50-Hz power system signal with chaotic noise. Initially, the chaotic oscillations are modeled and simulated with the FDO using the MATLAB programming language. The MEKF and EKF estimation of the distorted signals is compared with the undistorted power system signal by means of time series diagrams, Poincaré maps, and phase space diagrams. The undistorted power system signal in a regular region is shown in Figure 3.

In the case of chaotic ferroresonance, it is very challenging to accurately estimate the system signal. In this study, we have used the MEKF to detect and estimate chaotic oscillations. The forcing parameter γ defines the frequency of the chaotic oscillations in the system signal. In order to compare the performance of the MEKF and EKF, 2 different scenarios were studied. In the first case, the regular driving force of the FDO is used ($\gamma = 1.5$) without damping ($\delta = 0$). The chaotic oscillations of the power system signal for this case are shown in Figure 7.

To detect system signal properly, 2 parameters need to be estimated adaptively. The 1st parameter is the amplitude and the 2nd parameter is the frequency of the system signal. The corresponding amplitude and frequency estimation of the EKF is given in Figure 8. The estimated system frequency with the EKF is calculated as 50.06 Hz.

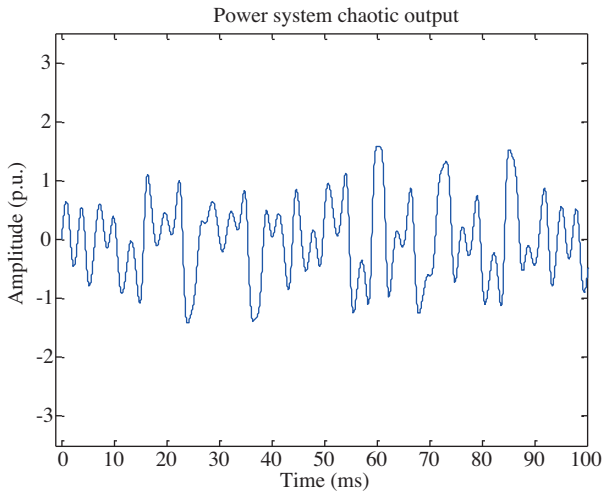

Figure 7. The chaotic oscillations of the power system signal due to the ferroresonance ($\gamma = 1.5$ and $\delta = 0$).

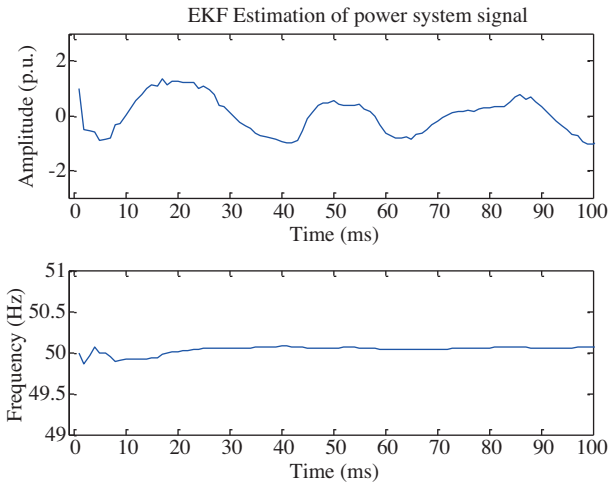

Figure 8. The amplitude and frequency estimation of the EKF for $\gamma = 1.5$ and $\delta = 0$.

The amplitude and frequency estimation of the MEKF for this scenario is given in Figure 9. The estimated system frequency with the MEKF is 50.01 Hz. The MEKF method has a slightly better estimation performance than the former EKF. To analyze the estimation performance of the proposed method in detail, the Poincaré map and phase space diagram of the estimation results are considered. The Poincaré map and phase space diagram of the EKF algorithm and MEKF algorithm are given in Figures 10 and 11, respectively. For these diagrams, the attractor characteristics are not displayed; on the contrary, they resemble unforced regular oscillator output diagrams. In the second case, in order to increase the chaotic behavior of the system, a stronger driving force is employed for the FDO ($\gamma = 2.5$) without damping ($\delta = 0$). The chaotic oscillations of the power system signal for this case are given in Figure 12.

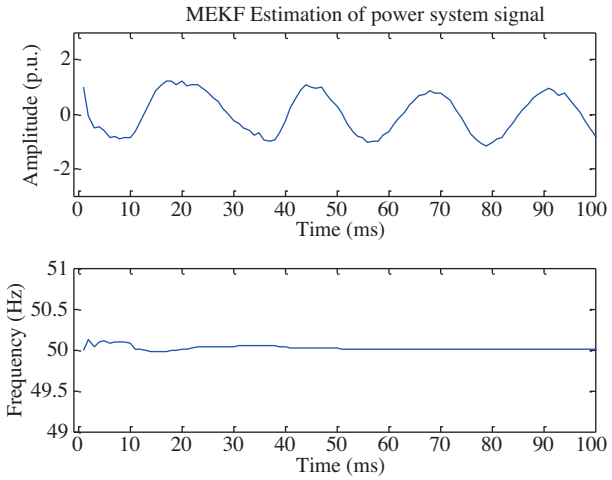

Figure 9. The amplitude and frequency estimation of the MEKF for $\gamma = 1.5$ and $\delta = 0$.

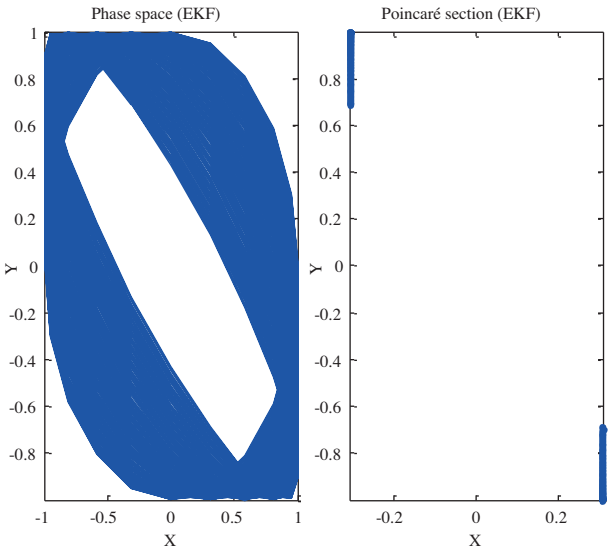

Figure 10. The phase space diagram and the Poincaré map of the EKF output for $\gamma = 1.5$ and $\delta = 0$.

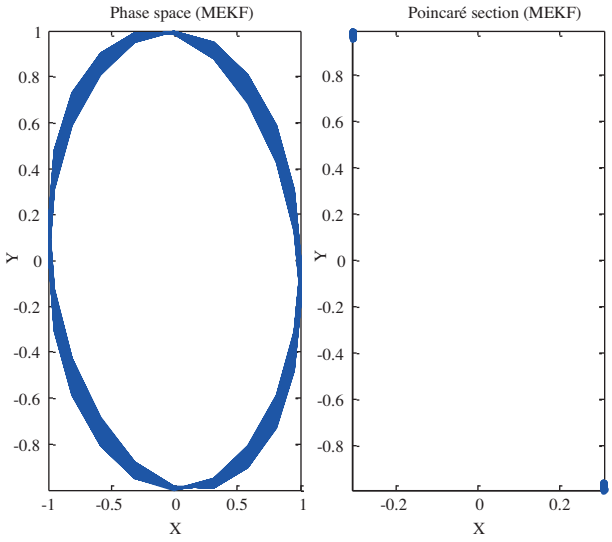

Figure 11. The phase space diagram and the Poincaré map of the MEKF output for $\gamma = 1.5$ and $\delta = 0$.

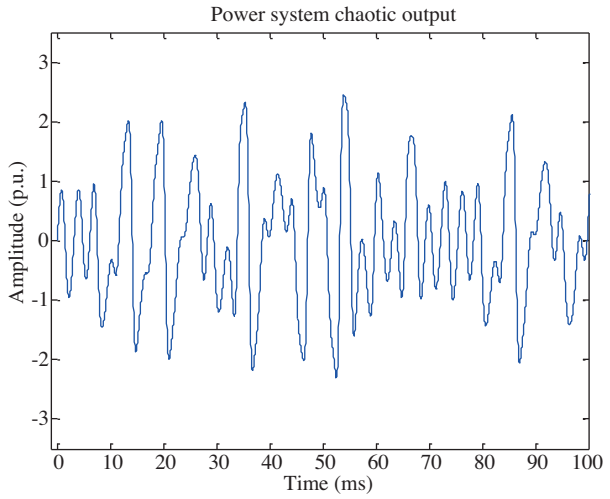

Figure 12. The chaotic oscillations of the power system signal due to the ferroresonance ($\gamma = 2.5$ and $\delta = 0$).

The amplitude and frequency estimation of the EKF is given in Figure 13. The estimated system frequency with the EKF for this scenario is 50.33 Hz. With the increasing driving force and chaoticness, the estimation performance is decreased considerably. However, the MEKF calculates the system frequency as 50.15 Hz (Figure 14), which is much better than that of the EKF. The filter output converges the fundamental frequency with a small error due to the increased driving force in 50 ms. The Poincaré map and the phase space diagram of the EKF and MEKF are given in Figures 15 and 16, respectively. With the less-spanned Poincaré map and phase space diagram, the MEKF displays more accurate estimation results than the EKF. Despite the increased chaotic behavior of the system, the MEKF output still tracks the system frequency and manifests the UDO output characteristics for $\gamma = 0$ and $\delta = 0$, like the undistorted power system signal.

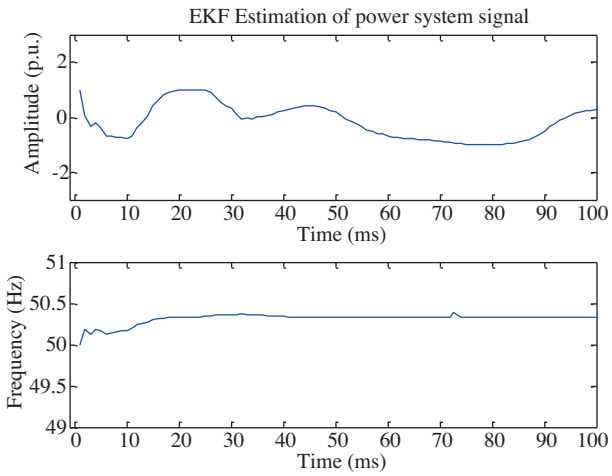

Figure 13. The amplitude and frequency estimation of the EKF for $\gamma = 2.5$ and $\delta = 0$.

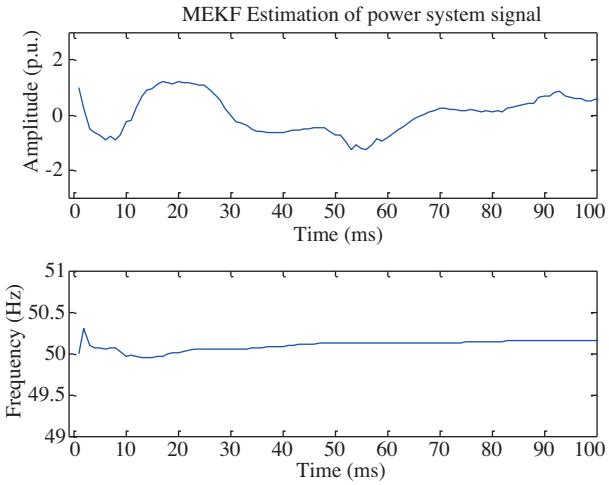

Figure 14. The amplitude and frequency estimation of the MEKF for $\gamma = 2.5$ and $\delta = 0$.

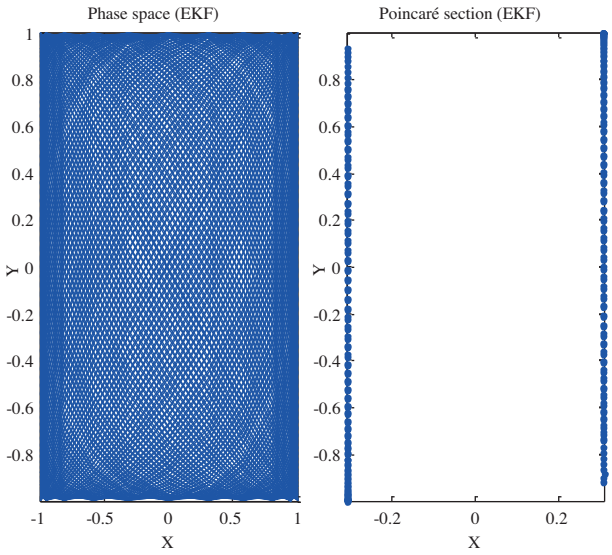

Figure 15. The phase space diagram and the Poincaré map of the EEKF output for $\gamma = 2.5$ and $\delta = 0$.

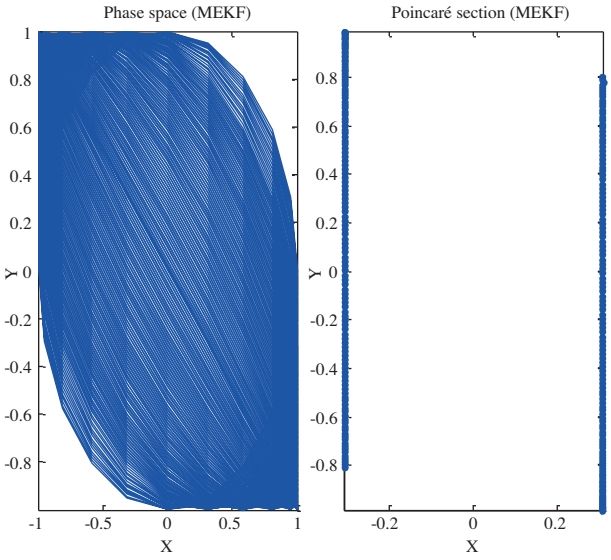

Figure 16. The phase space diagram and the Poincaré map of the MEKF output for $\gamma = 2.5$ and $\delta = 0$.

4. Conclusion

In this paper, a MEKF algorithm was proposed for frequency and amplitude estimation of chaotic oscillations in ferroresonance for a power system. The estimation performance of the MEKF method was compared with the former EKF method. The modification algorithm adjusts the covariance matrix adaptively according to the tracking performance of the MEKF. In this study in order to simulate the chaotic oscillations, the FDO was used. Two different cases were simulated depending on the forcing parameter (driving force) γ that defines the chaoticness of the system. The MEKF estimations of the chaotic oscillations under a regular driving force ($\gamma = 1.5$) exhibited satisfactory results. The filter detects the system frequency and amplitude accurately and rapidly with a 0.01-Hz error. In all of the cases, the MEKF method estimation performance was better than that of

the EKF method. The simulation of the Poincaré map and phase space diagram of the MEKF compared with the regular power system output diagrams indicated that the performance of the proposed algorithm under chaotic oscillations is suitable for the real-time detection of the chaoticness of the system. In the second case, an excessive over driving force ($\gamma = 2.5$) was employed to oscillate the system signal to simulate ferroresonance. In spite of the increasing chaoticness of the system, the MEKF still detects the frequency adaptively with an acceptable error (0.15 Hz). Moreover, the Poincaré map and phase space diagram of the MEKF resemble the regular oscillator diagrams, despite the increased randomness of the system. The proposed algorithm is suitable for real-time applications where highly chaotic behavior is monitored. Moreover, it can also be used to develop ferroresonance detection methodologies for power systems in the future.

References

[1] Z. Emin, B.A.T. Al Zahawi, Y.K. Tong, Y.K. Tong, M. Ugur, "Quantification of the chaotic behavior of ferroresonant voltage transformer circuits", IEEE Transactions on Circuits and Systems I: Fundamental Theory and Applications, Vol. 48, pp. 757–760, 2001.

[2] S. Yıldırım, T.Ç. Akıncı, S. Şeker, N. Ekren, "Determination of the characteristics for ferroresonance phenomenon in electric power systems", World Academy of Science, Engineering & Technology, Vol. 55, p. 108, 2009.

[3] S. Mosses, M.A.S. Masoum, "Modeling ferroresonance in single-phase transformer cores with hysteresis", Proceedings of the 8th WSEAS International Conference on System Science and Simulation in Engineering, pp. 246–250, 2009.

[4] S. Yıldırım, D. Bayram, T.Ç. Akıncı, S. Şeker, "Continuous wavelet transform for ferroresonance phenomenon in electric power systems", The 5th International Symposium on Wavelets to the World Problems, 2010.

[5] S. Çekli, C.P. Uzunoğlu, "Classification of chaotic circuit output patterns with probabilistic neural networks", IEEE 19th Conference on Signal Processing and Communications Applications, pp. 170–173, 2011.

[6] E. Tsonev, I. Simeonov, "Chaotic oscillations in ferroresonance circuits", Journal of BSUAE on Applied Electromagnetism, Vol. 6, pp. 66–81, 2004.

[7] A. Sanayei, "Controlling chaos in forced Duffing oscillator based on OGY method and generalized Routh-Hurwitz criterion", 2nd International Conference on Computer and Electrical Engineering, Vol. 2, pp. 591–595, 2009.

[8] A. Ersoy, A. Kuntman, "A study on influence of borax to polyester insulators", Turkish Journal of Electrical Engineering & Computer Sciences, Vol. 19, pp. 431–443, 2011.

[9] S. Çekli, C.P. Uzunoğlu, M. Uğur, "Adaptive frequency estimation of distorted power system signals using modified extended Kalman filter", Gazi University Journal of Science, Vol. 24, pp. 85–89, 2011.

[10] D. Zwillinger, Handbook of Differential Equations, Academic Press, Boston, 1997.

[11] S. Wiggins, Introduction to Applied Nonlinear Dynamical Systems and Chaos, New York, Springer-Verlag, 1990.

[12] P.F. Driessen, "DPLL bit synchronizer with rapid acquisition using adaptive Kalman filtering techniques", IEEE Transactions on Communications, Vol. 42, pp. 2673–2675, 1994.